

# New Fluorous Bipyridine Ligands for Copper-Catalyzed Atom Transfer Radical Polymerization of Methyl Methacrylate in the Thermomorphic Mode

Norman Lu, Ching-Lung Lin, Tsung-Chi Chen

*Institute of Organic and Polymeric Materials, National Taipei University of Technology, Taipei 106, Taiwan*

Received 8 December 2007; accepted 24 March 2008

DOI 10.1002/app.28513

Published online 10 July 2008 in Wiley InterScience (www.interscience.wiley.com).

**ABSTRACT:** The atom transfer radical polymerization (ATRP) of methyl methacrylate (MMA) is often carried out under homogeneous conditions, so the residual metal catalyst in the polymer often influences the quality of the polymer and causes environmental pollution in the long run. Novel CuBr/4,4'-bis(R<sub>f</sub>CH<sub>2</sub>OCH<sub>2</sub>)-2,2'-bpy complexes (R<sub>f</sub> = *n*-C<sub>9</sub>F<sub>19</sub>, *n*-C<sub>10</sub>F<sub>21</sub>, or *n*-C<sub>11</sub>F<sub>23</sub>; 2,2'-bpy = 2,2'-bipyridine) are insoluble in toluene at room temperature yet readily dissolve in toluene at elevated temperatures to form homogeneous phases for use as catalysts in the ATRP reaction, and the Cu complexes

precipitate again upon cooling. The CuBr/4,4'-bis(*n*-C<sub>9</sub>F<sub>19</sub>CH<sub>2</sub>OCH<sub>2</sub>)-2,2'-bpy system produced the best results (e.g., polydispersity index by gel permeation chromatography = 1.26–1.41), in that the residual Cu content in the polymer was as low as 19.3 ppm when the ATRP of MMA was carried out in the thermomorphic mode. © 2008 Wiley Periodicals, Inc. *J Appl Polym Sci* 110: 2531–2537, 2008

**Key words:** atom transfer radical polymerization (ATRP); catalysts; gel permeation chromatography (GPC)

## INTRODUCTION

The search for recoverable catalysts is a major task in the field of catalysis.<sup>1</sup> Atom transfer radical polymerization (ATRP)<sup>2</sup> is an area of intense research because of the possibility of controlling the molecular weight, polydispersity index (PDI), and end-functionalized synthesis of the final polymer. ATRP typically uses one metal/ligand complex to mediate one growing polymer chain to achieve reasonable reaction rates. Consequently, the resulting polymer is often colored because of the residual metal.

Indeed, one of the limitations of ATRP for industrial development is the presence of a residual transition-metal catalyst in the final polymer, which is likely to cause environmental problems. Different purification methods have been proposed in the recent literature, but the most developed method is the immobilization of the ATRP catalyst onto organic or inorganic polymeric supports.<sup>3</sup> However, immobilized catalysts usually do not effectively

mediate the polymerization process. This may be attributed to a number of factors, including poor contact of the growing radical chain end to the deactivating species<sup>4</sup> and catalyst heterogeneity.<sup>5</sup>

Recently, more efficient heterogeneous,<sup>6</sup> two-component heterogeneous/homogeneous,<sup>7</sup> and thermoresponsive catalysts<sup>8</sup> have been reported. However, the relatively tedious preparation and recovery procedures might pose limitations for industrial applications. In 1999, Vincent et al.<sup>9</sup> reported the first example of a recyclable molecular catalyst for ATRP based on a fluorous biphasic system, which proved to be effective for catalyst recovery with the ATRP method. However, its expensive cost and low efficiency in controlling the molar masses of the polymers prevent it from being used in industrial applications.<sup>10</sup>

Gladysz and coworkers<sup>11,12</sup> recently introduced the solubility-based thermomorphic properties of heavy fluorous catalysts in organic solvents as a new strategy for performing homogeneous catalysis without a fluorous solvent. Catalyst recovery has been achieved by liquid/solid separation.<sup>13</sup> Vincent et al.<sup>14</sup> in 2004 also reported the solubility-based thermomorphic properties of a nonfluorous catalyst that is based on a long hydrocarbon chain (C<sub>8</sub>H<sub>17</sub>). Inspired by these works, we have been wondering if this approach could be extended, for particular cases, to catalysts carrying O-perfluoroalkylated 2,2'-bipyridine (2,2'-bpy) ligands. Reported here is

Additional Supporting Information may be found in the online version of this article.

Correspondence to: N. Lu (normanlu@ntut.edu.tw).

Contract grant sponsor: National Science Council of Taiwan; contract grant number: 95-2113-M-027-002.

*Journal of Applied Polymer Science*, Vol. 110, 2531–2537 (2008)  
© 2008 Wiley Periodicals, Inc.

fluorous 2,2'-bpy for use in the copper (Cu)-catalyzed ATRP of methyl methacrylate (MMA) in the thermomorphic mode and simple recovery by solid/liquid decantation at room temperature. Using this approach, we have also successfully demonstrated that the Cu-catalyzed aerobic oxidation of alcohols<sup>15</sup> can proceed well under such conditions.

## EXPERIMENTAL

### General

Gas chromatography/mass spectrometry (GC/MS) data were obtained with an Agilent 6890 series gas chromatograph (Santa Clara, CA) with a series 5973 mass selective detector and an Agilent HP-1 column (30 m × 0.250 mm × 1 μm). Infrared spectra were obtained on a PerkinElmer RX I Fourier transform infrared (FTIR) spectrometer (Waltham, MA). The residual Cu content was determined with inductively coupled plasma/mass spectrometry (ICP-MS). The NMR spectra were recorded with a Bruker AM 500 (Rheinstetten, Germany) and JEOL AM 200 (Peabody, MA) with 5-mm sample tubes. Chemical shifts of the NMR spectra were recorded in parts per million with the downfield positive. The residual peaks of deuterated solvents (deuterated dimethylformamide, CDCl<sub>3</sub>, etc.) were used as the reference peaks for both <sup>1</sup>H- and <sup>13</sup>C-NMR spectra, and Freon 11 (CFCl<sub>3</sub>) was used for <sup>19</sup>F-NMR spectra.

Gel permeation chromatography (GPC) was used to determine the polymer molecular weights and molecular weight distributions (PDIs) with polystyrene standards (Polysciences Corp., Niles, IL) to generate a universal calibration curve for poly(methyl methacrylate) (PMMA). These measurements were made with a Waters GPC-150CV size exclusion chromatographer (Milford, MA) equipped with a Waters refractive-index detector and two 6.0 × 150 mm high-resolution GPC HspgelHR columns (molecular weight ranges: 1 × 10<sup>2</sup> to 1 × 10<sup>3</sup> and 5 × 10<sup>2</sup> to 7 × 10<sup>5</sup>) at a flow rate of 0.5 mL/min with tetrahydrofuran (THF) or toluene as the mobile phase at 35°C. Data were recorded and processed with the Waters software package.

### Preparation of 4,4'-bis(R<sub>f</sub>CH<sub>2</sub>OCH<sub>2</sub>)-2,2'-bpy [R<sub>f</sub> = *n*-C<sub>9</sub>F<sub>19</sub> (1a), *n*-C<sub>10</sub>F<sub>21</sub> (1b), or *n*-C<sub>11</sub>F<sub>23</sub> (1c)]

#### General procedure

Thirty percent CH<sub>3</sub>ONa/CH<sub>3</sub>OH (15.0 mmol) and R<sub>f</sub>CH<sub>2</sub>OH (15.0 mmol) were charged into a round-bottom flask and then continuously stirred under an N<sub>2</sub> atmosphere at 65°C for 4 h before CH<sub>3</sub>OH was vacuum-removed to drive the reaction to the fluorinated alkoxide side. The resulting fluorinated alkoxide (15.0 mmol) was then dissolved in 20 mL of dry

THF, and 4,4'-bis(BrCH<sub>2</sub>)-2,2'-bpy (5.8 mmol, 2.0 g) was added. The mixture was brought to refluxing for 4 h, and the completeness of the reaction was checked by the sampling of the reaction mixtures and analysis of the aliquots with GC/MS. The product was purified by vacuum sublimation to obtain white solids. The vacuum level was 0.1 Torr, and the sublimation temperature was 50°C above its melting point.

#### 1a

Yield (sublimed): 72%. <sup>1</sup>H-NMR (500 MHz, *d*-toluene, δ): 8.51 (2H, d, <sup>3</sup>J<sub>HH</sub> = 4.7 Hz, H<sub>6</sub>), 8.53 (2H, s, H<sub>3</sub>), 6.93 (2H, d, <sup>3</sup>J<sub>HH</sub> = 4.7 Hz, H<sub>5</sub>), 4.18 (4H, s, bpy-CH<sub>2</sub>), 3.56 (4H, t, <sup>3</sup>J<sub>HF</sub> = 13.5 Hz, CF<sub>2</sub>CH<sub>2</sub>). <sup>19</sup>F-NMR (470.5 MHz, *d*-toluene, δ): -80.8 (3F), -118.7 (2F), -121.8 (8F), -122.6 (2F), -123.2 (2F), -125.6 (2F). <sup>13</sup>C-NMR (113 MHz, *d*-toluene, δ): 73.5 (bpy-CH<sub>2</sub>), 68.2 (CH<sub>2</sub>CF<sub>2</sub>), 157.2, 149.9, 146.9, 121.9, 119.7 (bpy), 105.0–116.0 (C<sub>8</sub>F<sub>17</sub>). GC/MS (*m/z*; electron impact): 682 (M<sup>+</sup>-OCH<sub>2</sub>C<sub>9</sub>F<sub>19</sub>), 198 (C<sub>5</sub>H<sub>3</sub>NCH<sub>2</sub>C<sub>5</sub>H<sub>3</sub>NCH<sub>2</sub>O<sup>+</sup>), 183 (C<sub>5</sub>H<sub>3</sub>NCH<sub>2</sub>C<sub>5</sub>H<sub>3</sub>NCH<sub>3</sub><sup>+</sup>), 91 (C<sub>5</sub>H<sub>3</sub>NCH<sub>2</sub><sup>+</sup>). FTIR (cm<sup>-1</sup>): 1599, 1463 (vbpy, m), 1208.7, 1144.7 (vCF<sub>2</sub>, vs). mp: 125–128°C.

#### 1b

Yield (sublimed): 65%. <sup>1</sup>H-NMR (500 MHz, CDCl<sub>3</sub> at 60°C to increase the solubility, δ): 8.69 (2H, d, <sup>3</sup>J<sub>HH</sub> = 5.1 Hz, H<sub>6</sub>), 8.40 (2H, s, H<sub>3</sub>), 7.38 (2H, d, <sup>3</sup>J<sub>HH</sub> = 4.2 Hz, H<sub>5</sub>), 4.80 (4H, s, bpy-CH<sub>2</sub>), 4.06 (4H, t, <sup>3</sup>J<sub>HF</sub> = 13.3 Hz, CF<sub>2</sub>CH<sub>2</sub>). <sup>19</sup>F-NMR (470.5 MHz, CDCl<sub>3</sub> at 60°C, δ): -80.7 (3F), -119.3 (2F), -121.7 (6F), -121.8 (4F), -122.6 (2F), -123.1 (2F), -126.0 (2F). <sup>13</sup>C-NMR (113 MHz, CDCl<sub>3</sub> at 60°C, δ): 73.1 (bpy-CH<sub>2</sub>), 68.1 (CH<sub>2</sub>CF<sub>2</sub>), 154.1, 149.4, 144.7, 122.2, 119.8 (bpy), 105.5–116.2 (C<sub>10</sub>F<sub>21</sub>). GC/MS (*m/z*; electron impact): 732 (M<sup>+</sup>-OCHC<sub>10</sub>F<sub>21</sub>), 198 (C<sub>5</sub>H<sub>3</sub>NCH<sub>2</sub>C<sub>5</sub>H<sub>3</sub>NCH<sub>2</sub>O<sup>+</sup>), 183 (C<sub>5</sub>H<sub>3</sub>NCH<sub>2</sub>C<sub>5</sub>H<sub>3</sub>NCH<sub>3</sub><sup>+</sup>), 91 (C<sub>5</sub>H<sub>3</sub>NCH<sub>2</sub><sup>+</sup>). FTIR (cm<sup>-1</sup>): 1602.4, 1561.7 (vbpy, m), 1215.0, 1150.5 (vCF<sub>2</sub>, vs). mp: 140–142°C.

#### 1c

Yield (sublimed): 63.2%. <sup>1</sup>H-NMR (500 MHz, *d*-toluene at 90°C to increase the solubility, δ): 8.51 (2H, d, <sup>3</sup>J<sub>HH</sub> = 5.1 Hz, H<sub>6</sub>), 8.52 (2H, s, H<sub>3</sub>), 6.93 (2H, d, <sup>3</sup>J<sub>HH</sub> = 4.2 Hz, H<sub>5</sub>), 4.19 (4H, s, bpy-CH<sub>2</sub>), 3.59 (4H, t, <sup>3</sup>J<sub>HF</sub> = 13.3 Hz, CF<sub>2</sub>CH<sub>2</sub>). <sup>19</sup>F-NMR (470.5 MHz, *d*-toluene at 90°C, δ): -81.1 (3F), -119.3 (2F), -121.7 (12F), -122.6 (2F), -123.1 (2F), -125.8 (2F). <sup>13</sup>C-NMR (113 MHz, *d*-toluene at 90°C, δ): 73.5 (bpy-CH<sub>2</sub>), 68.2 (CH<sub>2</sub>CF<sub>2</sub>), 157.2, 149.9, 146.9, 121.8, 119.6 (bpy), 105.0–116.0 (C<sub>10</sub>F<sub>23</sub>). GC/MS (*m/z*; electron impact): 732 (M<sup>+</sup>-OCHC<sub>11</sub>F<sub>23</sub>), 198 (C<sub>5</sub>H<sub>3</sub>NCH<sub>2</sub>C<sub>5</sub>H<sub>3</sub>NCH<sub>2</sub>O<sup>+</sup>), 183 (C<sub>5</sub>H<sub>3</sub>NCH<sub>2</sub>C<sub>5</sub>H<sub>3</sub>NCH<sub>3</sub><sup>+</sup>),

91 ( $C_5H_3NCH_2^+$ ). FTIR ( $cm^{-1}$ ): 1599.4, 1463.7 (vbpy, m), 1208.0, 1150.5 ( $\nu_{CF_2}$ , vs). mp: 147–150°C.

#### Temperature dependence of CuBr/1a solubility in toluene

The solubility of Cu complexes was evidenced by a recrystallization experiment. CuBr (0.05 mmol, 7.15 mg) and ligand **1a** (0.10 mmol, 118 mg) were heated in toluene (5 mL) at 80°C to form an approximately 10 mM solution (a few drops of dimethylformamide were helpful for speeding up this dissolving process). A portion of the 10 mM solution was diluted 500 times to form an approximately 0.02 mM solution. Both were clear solutions at  $80 \pm 3^\circ C$ . These two solutions (10 and 0.02 mM), however, gave precipitates at 20°C. This suggests that the solubility of CuBr/1a increased 500-fold ( $10/0.02 = 500$ ) when the temperature was raised from 20 to 80°C.

#### ATRP of MMA in the thermomorphic mode

Under a nitrogen atmosphere, CuBr (0.10 mmol, 14.3 mg) and the ligand (0.20 mmol; 236 mg of **1a**, 246 mg of **1b**, or 256 mg of **1c**) were charged into a 50-mL Schlenk flask and followed by FC-77 (4 mL), methoxyperfluorobutane (HFE-7100) (2 mL), and acetonitrile (3 mL). The mixture was stirred for 16 h to form the dark-colored Cu complex (CuBr/1a, CuBr/1b, or CuBr/1c), and then the solvents in the material were removed by vacuum to yield a solid. The resulting solid (CuBr/1a, CuBr/1b, or CuBr/1c) was then used as a catalyst for the polymerization steps.

To the flask containing the Cu complex were introduced MMA (10 mmol, 1.0 g) and toluene (5.5 mL). After three freeze–thaw cycles, the temperature was raised to 80°C before the slow addition of the ethyl 2-bromoisobutyrate initiator (0.1 mmol, 19.5 mg), which was predissolved in a small amount of toluene. This addition was accomplished with a degassed syringe over a period of 5 min. Periodically, aliquots of the reaction mixture were taken with a degassed syringe for analysis by  $^1H$ -NMR to calculate the conversion. The mixture became a green solution at the end of the reaction. Then, the product mixture was frozen to  $-10^\circ C$ . The used solid complex (CuBr/1a, CuBr/1b, or CuBr/1c) was separated from the solution by decantation. The PMMA product was obtained either by evacuation of the solvents or by precipitation when excess methanol was added. The molecular weight of the resulting PMMA was determined by GPC and  $^1H$ -NMR; the residual Cu content was analyzed by ICP–MS.

$^1H$ -NMR (500 MHz,  $CDCl_3$ ,  $\delta$ , ppm): 0.50–1.20 (m,  $-CCH_3$ ), 1.60–2.05 (m br,  $-CH_2-$ ), 3.57 (s br,  $-OCH_3$ ). (The spectrum is shown in Fig. S.a in the supplementary material.)

#### Synthesis of the block copolymer

A flask containing the Cu complex (CuBr/1a; 0.1 mmol) synthesized in a way similar to those used previously for the MMA ATRP experiments was prepared. Then, the PMMA macroinitiator [0.062 mmol, 0.459 g; weight-average molecular weight ( $M_w$ ) = 7411; PDI = 1.26], dissolved in 3 mL of toluene, and butyl methacrylate (BMA; 7.0 mmol, 1.00 g), dissolved in 2 mL of toluene, were added to the flask under a nitrogen atmosphere. The reaction mixture was then heated at 80°C for 24 h during polymerization. After catalyst precipitation and then evaporation of the volatiles, the amount of the obtained polymer was 1.309 g. (For the GPC analysis, a small amount of the resulting polymer was redissolved in dimethylformamide and was precipitated by the addition of excess methanol.) The yield of the copolymer was about 85%, and its number-average molecular weight ( $M_n$ ) was 17,838 (PDI = 1.51; theoretical  $M_n = 19,481$ ), as determined by GPC. The molecular weight estimated by  $^1H$ -NMR data was 18,461 (its spectrum is shown in Fig. S.b in the supplementary material).

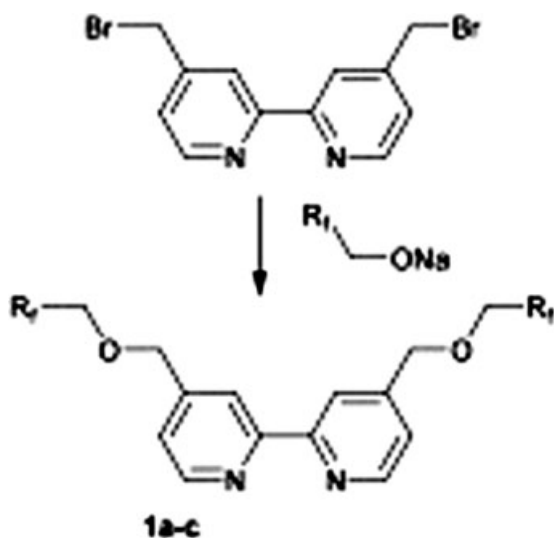
$^1H$ -NMR (200 MHz,  $CDCl_3$ ,  $\delta$ , ppm): 0.50–2.10 (m br,  $-CCH_3$ ,  $-CH_2-$ ,  $OCH_2CH_2CH_2CH_3$ ), 3.57 (s br,  $-OCH_3$ ), 3.92 (s br,  $-OCH_2CH_2-$ ).

#### Reverse ATRP of MMA

Into a 50-mL Schlenk flask, under an  $N_2$  atmosphere, the recovered Cu complex from the reaction of ATRP of MMA and toluene were charged, and they were followed by 200 equiv of MMA. The flask was submerged into an 80°C oil bath. 2,2'-Azobisisobutyronitrile, predissolved in a small amount of toluene, was added to the mixture, and then the polymerization was started. After 48 h, the polymerization products were analyzed by the  $^1H$ -NMR method. The yield was 81%.

## RESULTS AND DISCUSSION

The preparation of fluoro-ponytailed 2,2'-bpy ligands started with the deprotonation of readily available fluororous alkanols ( $R_fCH_2OH$ , where  $R_f = n-C_9F_{19}$ ,  $n-C_{10}F_{21}$ , or  $n-C_{11}F_{23}$ ). They were treated with  $CH_3ONa$  solutions (30% in  $CH_3OH$ ) to give the corresponding alkoxides. As shown in Scheme 1, the alkoxides were then reacted with 4,4'-bis(Br $CH_2$ )-2,2'-bpy<sup>16–18</sup> to give rise to **1a–1c**. Novel ligands of this type were successfully synthesized by our group and used in applications elsewhere also.<sup>19–21</sup> The Cu complexes CuBr/1a, CuBr/1b, and CuBr/1c could be generated *in situ* through the stirring of ligands **1a–1c**, respectively, with CuBr in a molar ratio of 2 : 1 at room temperature under nitrogen. The solubility



Scheme 1 Syntheses of ligands 1a–1c.

of the CuBr/1a, CuBr/1b, and CuBr/1c complexes in toluene increased about 500-fold when the temperature was raised from 20 to 80°C. Because of the availability of the fluorinated alcohols, ligands 1a–1c were found to be useful for the ATRP of MMA in toluene in the thermomorphic mode.

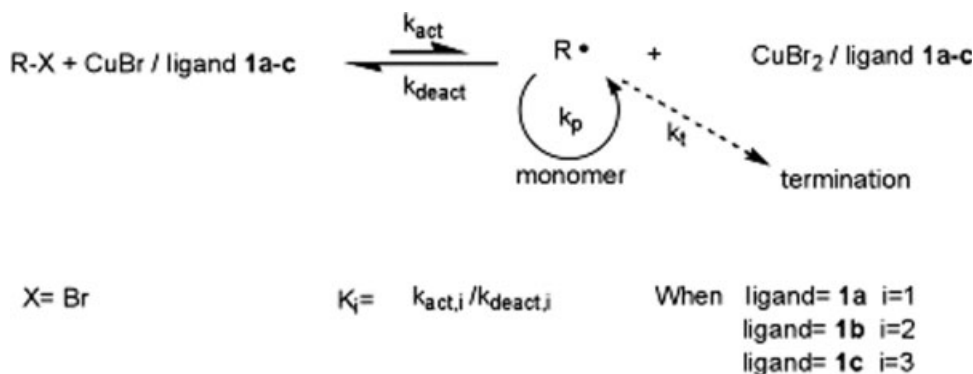
As mentioned previously, the CuBr/1a, CuBr/1b, and CuBr/1c systems were prepared through the reaction of CuBr with 2 equiv of 1a–1c, respectively. The mixtures were stirred in the cosolvent (acetonitrile/FC-77/HFE-7100) for 8 h under a nitrogen atmosphere. The CuBr/1a, CuBr/1b, and CuBr/1c complexes, which were sensitive to molecular oxygen, were easily isolated as dark-colored solids under a nitrogen atmosphere. The ATRP of MMA was carried out in toluene at 80°C with ethyl 2-bromoisobutyrate as an initiator and CuBr/1a, CuBr/1b, or CuBr/1c as the catalyst.

The ATRP mechanism, shown in Scheme 2, includes the equilibrium of Cu complexes and the polymerization/termination reactions. The order of

the  $K$  values of the three equilibria should be  $K_1 < K_2 < K_3$  because once the CuBr<sub>2</sub>/ligand complexes 1a–1c are formed (on the right), it is most difficult one for the bulkiest species, CuBr<sub>2</sub>/1c, to sterically undergo the backward reaction to return to the complex CuBr/1c (on the left). It is already known that ligands from the three systems CuBr<sub>2</sub>/1a, CuBr<sub>2</sub>/1b, and CuBr<sub>2</sub>/1c have similar electronic effects.<sup>15</sup>

The preformed complexes CuBr/1a, CuBr/1b, and CuBr/1c were soluble at 80°C in the early stages of the reaction, and this allowed the precise control of the amount of catalyst present in each solution to ensure an efficient initiation step. All three CuBr/1a-, CuBr/1b-, and CuBr/1c-catalyzed polymerizations proceeded at 80°C with first-order kinetics with respect to the monomer concentrations. The CuBr/1a, CuBr/1b, and CuBr/1c systems took 15, 8, and 5 h to reach the 80% conversion level, respectively, as shown in Figure 1. The polymerization rates in decreasing order were CuBr/1c > CuBr/1b > CuBr/1a. Because the CuBr/1c system had the largest value of  $K_3$ , the concentration of radicals ( $R\cdot$ ) generated by the CuBr/1c system was then the greatest. The CuBr/1c system also had the longest fluorinated chain among the three systems studied.  $\ln(M_0/M)$  was linearly dependent on time for all three systems. Accordingly, the slopes of  $\ln(M_0/M)$  versus time in decreasing sequence were also CuBr/1c > CuBr/1b > CuBr/1a.

Shown in Figure 2,  $M_n$  and PDI of the resulting PMMA from the CuBr/1a, CuBr/1b, and CuBr/1c systems are plotted against the conversion; the initiator having been added within 5 min during the polymerizations. The CuBr/1a-catalyzed ATRP of MMA produced the lowest PDI, controlled molecular weight, and initiation efficiency. The CuBr/1a-catalyzed reaction was the slowest among the three systems, taking about 24 h to reach the 90% conversion level. The relatively high concentration of radicals ( $R\cdot$ ) in the CuBr/1b- or CuBr/1c-catalyzed ATRP made the control of the molecular weight and molecular weight distribution not as good (i.e., less



Scheme 2 Mechanism of ATRP ( $k_{act}$  = rate constant of activation;  $k_{deact}$  = rate constant of deactivation).

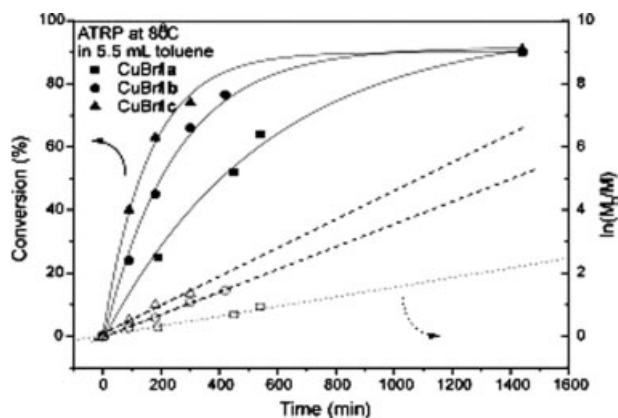


**Figure 1** Kinetic plot of CuBr/1a-, CuBr/1b-, and CuBr/1c-catalyzed ATRP of MMA ( $[\text{CuBr}/1\text{a-1c}] = [\text{initiator}] = 0.1 \text{ mmol}$ ,  $[\text{MMA}] = 10 \text{ mmol}$ ): (■, □) CuBr/1a, (●, ○) CuBr/1b, and (▲, △) CuBr/1c.

narrow) as that obtained in the CuBr/1a-catalyzed ATRP.

In addition to the theoretical  $M_n$  values, the plots of the molecular weight versus the conversion for the CuBr/1a-catalyzed ATRP with three different methods are shown in Figure 3. In the first method, the initiator was added to the reaction mixture within 5 min to ensure the generation of enough radicals at the beginning of the initiation. The plot of  $M_n$  versus the conversion from this method was linear and close to the theoretical prediction. This method showed good control of the molar masses of the polymers, with fairly narrow PDIs for the resulting PMMA in the range of 1.26–1.41. The initiation efficiency of the CuBr/1a system was also very close to 100%. Furthermore, the second method was the halogen exchange technique, with the addition of CuCl instead of CuBr to mediate the reaction.<sup>22</sup> Lastly, the third method was the addition of the 10%

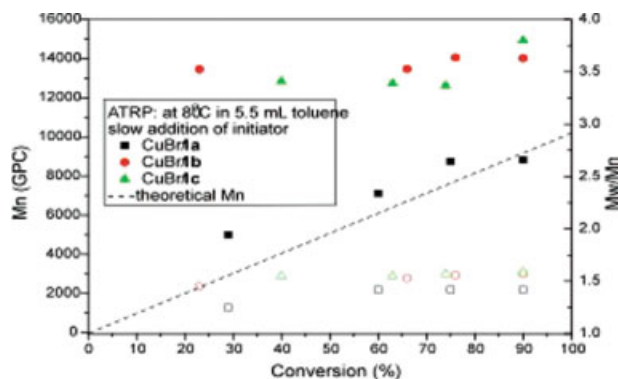


**Figure 2** Plot of the molecular weight and PDI versus the conversion for CuBr/1a, CuBr/1b, and CuBr/1c systems ( $[\text{CuBr}/1\text{a-1c}] = [\text{initiator}] = 0.1 \text{ mmol}$ ,  $[\text{MMA}] = 10 \text{ mmol}$ ): (■, □) CuBr/1a, (●, ○) CuBr/1b, and (▲, △) CuBr/1c. [Color figure can be viewed in the online issue, which is available at [www.interscience.wiley.com](http://www.interscience.wiley.com).]

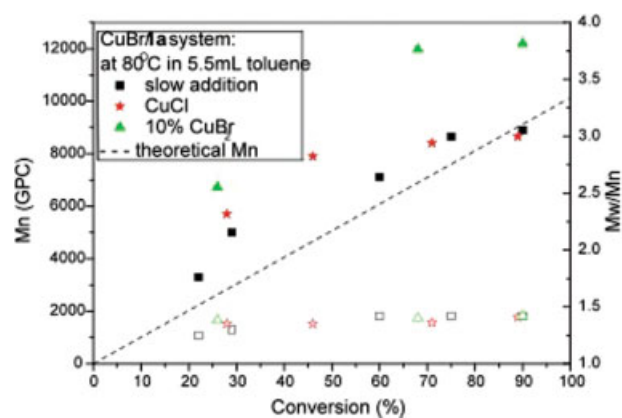


**Figure 3** Three methods for CuBr/1a-catalyzed ATRP of MMA ( $[\text{CuBr}/1\text{a-1c}] = [\text{initiator}] = 0.1 \text{ mmol}$ ,  $[\text{MMA}] = 10 \text{ mmol}$ ): (■, □) the addition of the initiator in 5 min, (★, ☆) halogen exchange by the addition of CuCl, and (▲, △) the addition of the 10% deactivating agent CuBr<sub>2</sub>. [Color figure can be viewed in the online issue, which is available at [www.interscience.wiley.com](http://www.interscience.wiley.com).]

deactivating agent, CuBr<sub>2</sub>, to control the polymerization.<sup>23</sup> As shown in Figure 3, the PDI and initiation efficiency results of the second and third methods were not as good as those of the first method for CuBr/1a-catalyzed ATRP.

As shown in Figure 4, during the workup, the product mixtures were cooled to  $-10^\circ\text{C}$  in a freezer, and then the precipitated Cu catalyst (the quick precipitation of the Cu catalyst was sometimes achieved by centrifugation) was easily separated from the product mixtures by filtration. The recovery of the used CuBr/1a, CuBr/1b, and CuBr/1c complexes was greater than 99%. The colorless filtrate, after evaporation of the volatiles, yielded PMMA as a white, glassy solid. A block copolymer consisting of

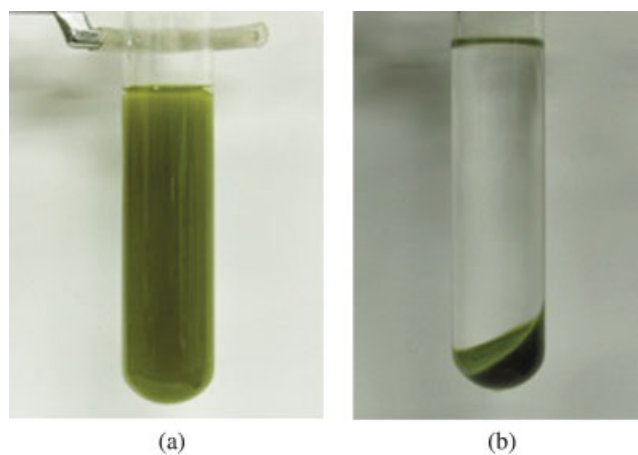


**Figure 4** Separation of the Cu catalyst from the product (PMMA) solution: (a) the solution immediately after polymerization and (b) the precipitation of the Cu catalyst after cooling. [Color figure can be viewed in the online issue, which is available at [www.interscience.wiley.com](http://www.interscience.wiley.com).]

MMA units as the first block and BMA as the second block was successfully prepared by the extension of the PMMA precursor. When the PMMA macroinitiator ( $M_n = 7411$ , PDI = 1.26) and BMA were used for the copolymerization, the block copolymer P(MMA-*b*-BMA) was successfully isolated. The preliminary results showed that the yield of P(MMA-*b*-BMA) was about 85%, and its  $M_n$  obtained from GPC was 17,838 (PDI = 1.51; theoretical  $M_n = 19,481$ ). These results successfully demonstrated the living character of the CuBr/**1a** catalytic system. The GPC data for the PMMA macroinitiator and its copolymer, P(MMA-*b*-BMA), are shown in Figure 5. It was known that some dead chains likely existed at the beginning of the polymerization. These dead chains would have lowered  $M_n$  and broadened the polymer molecular weight distribution, the value of which increased to PDI = 1.51 versus PDI = 1.26 from the PMMA macroinitiator. A shift of the GPC traces between the macroinitiator and the extended copolymer was also observed. In order to not inject residual metal into the GPC column, all the GPC samples were precipitated out by the addition of the excess methanol into the solution. Because the samples were well purified, a small amount of the PMMA macroinitiator might have been eliminated during this process. Furthermore, because of the relatively high conversion (85%), the number of dead chains should not have been too high. Thus, the tailing effect can be only slightly observed at the right edge of the dashed curve in Figure 5.

The ICP-MS data revealed the presence of very low residual Cu concentrations in PMMA obtained with CuBr/**1a**, CuBr/**1b**, and CuBr/**1c**. These results are summarized in Table I. Because the CuBr/**1a**-catalyzed ATRP of MMA demonstrated the best control of polymerizations in terms of the PDI, conversion

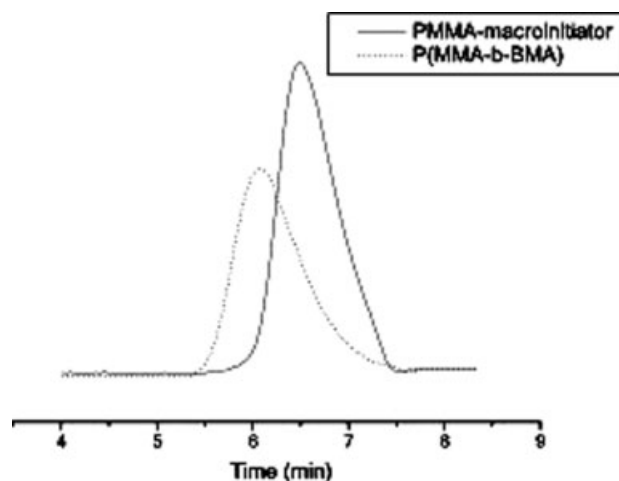


**Figure 5** GPC traces of the PMMA macroinitiator (PDI = 1.26,  $M_n = 7411$ ) and its copolymer P(MMA-*b*-BMA) (PDI = 1.51, theoretical  $M_n = 19,481$ ).

**TABLE I**  
Amount of Residual Cu Determined by ICP-MS

Cu catalyst	Residual Cu in PMMA (ppm) <sup>a</sup>	Recovery of used catalyst (%)
CuBr/ <b>1a</b>	19.3	99.73
CuBr/ <b>1b</b>	14.3	99.80
CuBr/ <b>1c</b>	39.4	99.45

<sup>a</sup> The detection limit of ICP-MS is 0.07 ppm.

and molecular weight relationship, and initiation efficiency, the data obtained with the CuBr/**1a**-catalyzed ATRP were used in sample calculations and comparisons. The 19.3 ppm residual Cu in PMMA detected by ICP-MS showed a low Cu content in comparison with 7044 ppm if all the catalyst remained in the polymer. Also indicated in Table I, the recovery was 99.73% for the used CuBr/**1a** catalyst. Furthermore, 19.3 ppm was an order of magnitude lower than the value of 200 ppm reported earlier for a nonfluorous thermoresponsive system.<sup>14</sup> The recovered green CuBr/**1a** complex was difficult to reduce for recycling. Nonetheless, we found that this used complex could be employed as a catalyst again by way of reverse ATRP of MMA. Preliminary results showed that PMMA made by reverse ATRP had a molecular weight of approximately 20,000, and its yield was close to 81%. Alternatively, the expensive fluorinated ligands **1a**–**1c** could be recycled with 74–84% yields if the recovered Cu complexes, dissolved in a fluorinated solvent (e.g., FC 77), were treated with an excess amount of aqueous ethylene diamine tetraacetic acid and stirred at room temperature for several days. The demetalated fluorinated ligands **1a**–**1c** could be recovered in the bottom layer (fluorinated solvent), with the top aqueous layer containing the ethylene diamine tetraacetic acid chelated Cu metal ions.

## CONCLUSIONS

A series of novel fluorinated 2,2'-bpy ligands (**1a**–**1c**) were prepared with good yields and were easily purified by sublimation. For catalytic reactions performed in toluene, the introduction of CuBr/**1a**, CuBr/**1b**, and CuBr/**1c** catalysts with novel fluorinated 2,2'-bpy is likely a valuable strategy for obtaining colorless and low-Cu-containing living polymers without further purification steps. The advantages of the CuBr/**1a**, CuBr/**1b**, and CuBr/**1c** catalysts include good conversion for polymerization, the recovery of Cu complexes by simple filtration, and low residual metal in the polymer. All three catalysts (CuBr/**1a**, CuBr/**1b**, and CuBr/**1c**) perform effectively for the living ATRP of MMA in the thermomorphic mode. In particular, the CuBr/**1a**

system showed the best controlled polymerization, the narrowest PDI, and low residual metal content. These properties could make CuBr/**1a**-catalyzed ATRP one step closer to industrial applications.

R. L. Sobocinski is greatly appreciated for proof-reading the manuscript.

## References

1. Gladysz, J. A. *Chem Rev* 2002, 102, 3215.
2. Tsarevsky, N. V.; Matyjaszewski, K. *Chem Rev* 2007, 107, 2270.
3. Nguyen, J. V.; Jones, C. W. *J Catal* 2005, 232, 276.
4. Queffelec, J.; Gaynor, S. G.; Matyjaszewski, K. *Macromolecules* 2000, 33, 8629.
5. (a) Kickelbick, G.; Paik, H.-J.; Matyjaszewski, K. *Macromolecules* 1999, 32, 2941; (b) Haddleton, D. M.; Duncalf, D. J.; Kukulj, D.; Radigue, A. P. *Macromolecules* 1999, 32, 4769.
6. (a) Nguyen, J. V.; Jones, C. W. *Macromolecules* 2004, 37, 1190; (b) Shen, Y.; Zhu, S.; Zeng, F.; Pelton, R. H. *Macromolecules* 2000, 33, 5427; (c) Shen, Y.; Zhu, S.; Pelton, R. *Macromolecules* 2001, 34, 5812.
7. (a) Hong, S. C.; Paik, H.-J.; Matyjaszewski, K. *Macromolecules* 2001, 34, 5099; (b) Hong, S. C.; Matyjaszewski, K. *Macromolecules* 2002, 35, 7592; (c) Yang, J.; Ding, S.; Radosz, M.; Shen, Y. *Macromolecules* 2004, 37, 1728.
8. Shen, Y.; Zhu, S.; Pelton, R. *Macromolecules* 2001, 34, 3182.
9. De Campo, F.; Lastecoueres, D.; Vincent, J.-M.; Verlhac, J.-B. *J Org Chem* 1999, 64, 4969.
10. Haddleton, D. M.; Jakson, S. G.; Bon, S. A. F. *J Am Chem Soc* 2000, 122, 1542.
11. Wende, M.; Meier, R.; Gladysz, J. A. *J Am Chem Soc* 2001, 123, 11490.
12. Wende, M.; Gladysz, J. A. *J Am Chem Soc* 2003, 125, 5861.
13. Shen, Z. Y.; Chen, Y. H.; Frey, H.; Stiriba, S.-E. *Macromolecules* 2006, 39, 2092.
14. Barre, G.; Taton, D.; Lastecoueres, D.; Vincent, J.-M. *J Am Chem Soc* 2004, 126, 7764.
15. Lu, N.; Lin, Y. C. *Tetrahedron Lett* 2007, 48, 8823.
16. Ciana, L. D.; Dressick, W. J.; Zelewsky, A. V. *J Heterocycl Chem* 1990, 27, 163.
17. Oki, A. R.; Morgan, R. J. *Synth Commun* 1995, 25, 4093.
18. Will, G.; Boschloo, G.; Rao, S. N.; Fitzmaurice, D. *J Phys Chem B* 1999, 103, 8067.
19. Lu, N.; Chen, S. C.; Chen, T. C.; Liu, L. K. *Tetrahedron Lett* 2008, 49, 371.
20. Lu, N.; Lin, Y. C.; Chen, J. Y.; Fan, C. W.; Liu, L. K. *Tetrahedron* 2007, 63, 2019.
21. Lu, N.; Chen, J. Y.; Fan, C. W.; Lin, Y. C.; Wen, Y. S.; Liu, L. K. *Polyhedron* 2007, 26, 3045.
22. (a) Matyjaszewski, K.; Wang, J. L.; Grimaud, T.; Shipp, D. A. *Macromolecules* 1998, 31, 1527; (b) Matyjaszewski, K.; Shipp, D. A.; Wang, J. L.; Grimaud, T.; Patten, T. E. *Macromolecules* 1998, 31, 6836.
23. Zhang, H.; Klumperman, B.; Ming, W.; Fischer, H.; van der Linde, R. *Macromolecules* 2001, 34, 6169.